Journal of Molecular Structure 967 (2010) 80–88

Contents lists available at ScienceDirect

Journal of Molecular Structure

journal homepage: www.elsevier.com/locate/molstruc

Crystal and molecular structure of the quinuclidine betaine with *p*-hydroxybenzoic acid complex studied by X-ray diffraction, DFT, FTIR, and NMR methods

Z. Dega-Szafran *, A. Katrusiak, M. Szafran

Faculty of Chemistry, Adam Mickiewicz University, ul. Grunwadzka 6, 60-780 Poznań, Poland

ARTICLE INFO

Article history:
Received 1 December 2009
Accepted 22 December 2009
Available online 29 December 2009

Keywords:
Quinuclidine betaine
4-Hydroxybenzoic acid
Hydrogen bonds
X-ray diffraction
DFT calculations
Spectroscopic studies

ABSTRACT

Quinuclidine betaine (1-carboxymethyl-1-azabicyclo[2.2.2]octane inner salt, QNB) forms a complex with *p*-hydroxybenzoic acid (HBA) at the 1:1 ratio. The crystals are triclinic, space group $P\bar{1}$, with two symmetry non-equivalent QNB·HBA complexes linked by a sequence of four O–H···O hydrogen bonds into a zigzag chain. Both oxygen atoms of the carboxylate groups of two QNB are linked with two HBA molecules through the COO···HOOC hydrogen bonds of 2.561(2), and 2.556(2) Å, and the COO···HO hydrogen bonds of 2.609(2) and 2.687(2) Å. A trio ABC band at ca. 2800, 2550, 1910 cm^{-1} observed in the FTIR spectrum is characteristic of a medium-strong hydrogen bond in carboxylic acids. The second-derivative IR spectrum confirms the presence of two non-equivalent C=O and two COO groups. The molecular structures of the 1:1 and 2:2 complexes have been optimized by the B3LYP/6-31G(d,p) approach. The experimental and predicted, by GIAO/B3LYP/6-31G(d,p), ^1H and ^{13}C chemical shifts correlate linearly.

1. Introduction

p-Hydroxybenzoic acid crystallizes as monohydrate in monoclinic space group $P2_1/a$ [1–3]. A pair of acid molecules is linked through the hydrogen bonds (2.678 Å) between carboxyl groups to form a dimer. The dimers are further hydrogen bonded between phenolic hydroxyl groups and water molecules. *p*-Hydroxybenzoic acid has been isolated from *Cinnamomum osmophloeum* leaves and identified by X-ray diffraction [4]. *p*-Hydroxybenzoic acid has two different proton-donor groups, COOH ($pK_{a1} = 4.67$) and OH ($pK_{a2} = 9.37$) [5]. The effect of substituent on the pK_a values of substituted benzoic acid has been examined using the DFT (density functional theory) calculations [6].

Recently, we have studied the effect of the hydroxyl group in benzoic acids, as an additional proton-donor group, in complexes with zwitterionic compounds, e.g. betaines [7–14]. The present paper is a continuation of that project. We have now extended our study on preparation and determination the structure of the complex of quinuclidine betaine (1-carboxymethyl-1-azabicyclo[2.2.2]octane inner salt, QNB) with *p*-hydroxybenzoic acid, HBA (Fig. 1), as well as on the structures optimized at the B3LYP/6-31G(d,p) level of theory and spectroscopic studies of this novel chemical compound.

2. Experimental

Quinuclidine betaine (1-carboxymethyl-1-azabicyclo[2.2.2]-octane inner salt, QNB) was prepared as described previously in Ref. [15]. The complex of QNB with the commercial *p*-hydroxybenzoic acid (HBA) was obtained by mixing the equimolar amounts of QNB and HBA in methanol. The solvent was evaporated and the solid product was precipitated upon addition of diethyl ether. The crystals were grown from an acetonitrile–methanol mixture (6:1), m.p. 153 °C. Analysis for $C_{16}H_{21}NO_5$; calcd.:%C, 62.53; %H, 6.69; %N, 4.56; found:%C, 62,48; %H, 6.79; %N, 4.36. The deuterated complex was prepared by threefold crystallization from D_2O.

The crystal structure of QNB·HBA was determined by X-ray diffraction, measured with a KUMA KM-4 CCD diffractometer [16,17]. The structure was solved by direct methods using SHELXS-97 [18] and refined on F^2 by full-matrix least-squares with the SHELXL-97 [19]. The numbering of atoms is shown in Fig. 2. The crystal data, details of data collection and structure refinement are given in Table 1, and the final atomic coordinates are listed in Table 2. The complete set of structural parameters in CIF format is available as an Electronic Supplementary Publication from the Cambridge Crystallographic Data Centre (CCDC 755370).

The DFT calculations were performed with the GAUSSIAN-03 program package [20]. The calculations employed the B3LYP exchange-correlation functional, which combines the hybrid exchange functional of Becke [21,22] with the gradient-correlation functional of Lee, Yang and Parr [23] and the split-valence polarized 6-31G(d,p) basis set [24]. The magnetic isotropic shielding

---

* Corresponding author. Tel.: +48 61 8291216; fax: +48 61 8291505.
E-mail address: degasz@amu.edu.pl (Z. Dega-Szafran).

0022-2860/$ - see front matter © 2009 Elsevier B.V. All rights reserved.
doi:10.1016/j.molstruc.2009.12.043

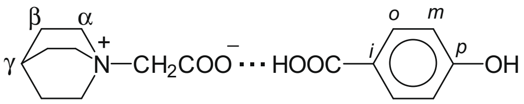

Fig. 1. Molecular structure of the 1:1 complex of quinuclidine betaine with *p*-hydroxybenzoic acid.

Table 1
Crystal data and structure refinement for the complex of quinuclidine betaine with *p*-hydroxybenzoic acid (1).

Empirical formula	$C_{32}H_{42}N_2O_{10}$
Formula weight	614.68
Temperature	293(2) K
Wavelength	1.54184 Å
Crystal system	Triclinic
Space group	$P\bar{1}$
Unit cell dimensions	
a	10.8266(4) Å
b	12.1538(5) Å
c	12.8039(5) Å
α	74.270(4)°
β	71.337(4)°
γ	77.574(4)°
Volume	1521.12(11) $Å^3$
Z	4
Calculated density	1.342 g/cm^3
Absorption coefficient	0.827 mm^{-1}
F(0 0 0)	656
Crystal size	0.3 × 0.2 × 0.1 mm
θ range for data collection	3.73–76.14°
Max/min. indices *h*, *k*, *l*	−13/12, −15/15, −10/16
Reflections collected/unique	11210/6095 [R_{int} = 0.0120]
θ_{Max}(°)/completeness (%)	76.14/95.8
Absorption correction	None
Refinement method	Full-matrix least-squares on F^2
Data/restraints/parameters	6095/0/565
Goodness-of-fit on F^2	1.022
Final *R*1/*wR*2 indices [$I > 2\sigma_I$]	0.0452/0.1181
*R*1/*wR*2 indices (all data)	0.0472/0.1197
Largest diff. peak and hole	0.302 and −0.213 e $Å^{-3}$

tensors were calculated with the standard GIAO/B3LYP/6-31G(d,p) (Gauge-Independent Atomic Orbital) approach using the conductor-like screening continuum solvation model (COSMO) [25].

FTIR spectrum was measured on a Bruker IFS 66v/S instrument, evacuated to avoid water and CO_2 absorptions, with the resolution of 2 cm^{-1}. The FTIR spectra were recorded in Nujol and Fluorolube suspensions using KBr plates. Each spectrum consisted of 64 scans.

The NMR spectra were recorded on a Varian Gemini 300 VT spectrometer operating at 300.07 and 75.46 MHz for ^1H and ^{13}C, respectively. The spectra were measured in DMSO-d_6 relative to internal standard of TMS.

3. Results and discussion

3.1. Crystal structure

The complex of quinuclidine betaine (QNB) with *p*-hydroxybenzoic acid (HBA) are formed at the 1:1 ratio and its structure (**1**) has been determined by X-ray diffraction. The crystals of **1** are triclinic, space group $P\bar{1}$. The structure with the atomic labels is shown in Fig. 2. Bond lengths, bond and torsion angles are given in Table 3. The complex **1** is built of two symmetry independent pairs of QNB·HBA (Figs. 2 and 3). Both oxygen atoms of the carboxylate group of each QNB moieties are involved in two hydrogen bonds with the COOH and OH groups of two neighboring HBA molecules (Fig. 3). The sequence of two COOH···OOC and O–H···OOC hydrogen bonds links the molecules into a chain extending along the crystal direction [1 1 0]. The shorter O–H···O hydrogen bonds, as expected, are formed between the COOH groups of HBA and COO^- groups of QNB: O(3)–H···O(1) and O(8)–H···O(6) of 2.591(2) and 2.556(2) Å, respectively. The hydroxyl group of the HBA molecules, as a weaker proton-donor, forms longer hydrogen bonds with QNB; O(10)–H···O(2) of 2.609(2) Å and O(5)–H···O(7)[a] of 2.687(2) Å [[a]Symmetry code: $x-1$, $y-1$, z) (Table 4). Similar arrangements of the molecules (betaines and HBA) were observed in the 1:1 complex of *N*-methylmorpholine betaine (MMB) with HBA [7] and in the complex of pyridine betaine with HBA [14], however, in the latter complex the COOH···OOC and OH···OOC hydrogen bonds are almost of the same length, 2.645(3) and 2.643(3) Å. The opposite situation has been observed in the complex of *N*-methylpiperidine betaine (MPB) with HBA, where the OH···OOC hydrogen bond is slightly shorter of 2.617(1) Å than the COOH···OOC bond of 2.622(1) Å, and two molecular pair of the MPB·HBA complexes are combined into a centrosymmetric dimer [8].

In the crystal structure of the complex investigated the piperidinium rings in both independent QNB moieties have a distorted-boat conformation. The same signs of torsion angles of the $N–CH_2–CH_2–CH$ bridges are characteristic of a propeller

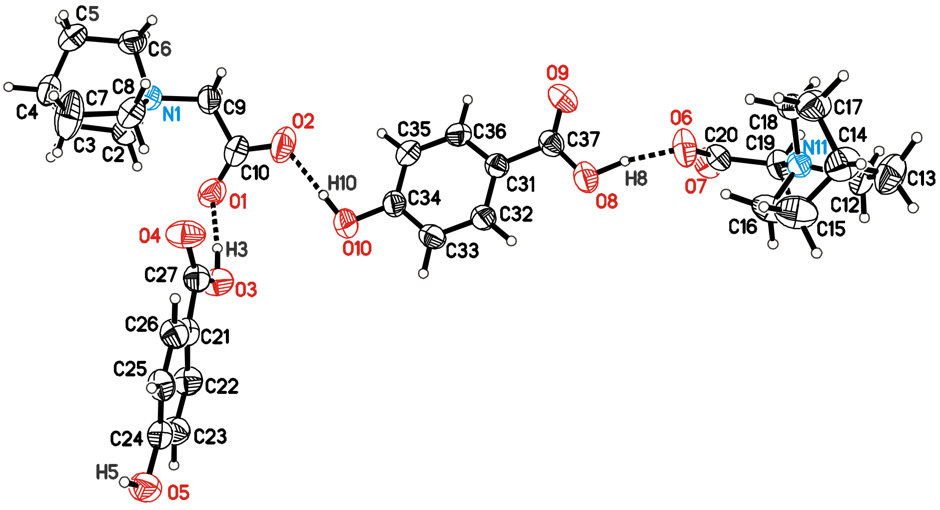

Fig. 2. The symmetry-independent part of the unit cell in the crystal structure of the complex of quinuclidine betaine with *p*-hydroxybenzoic acid. The hydrogen bonds are indicated as the dashed lines and the atomic vibrations are visualized as ellipsoids drawn at the 50% probability level.

Table 2
Atomic coordinates ($\times 10^4$) and equivalent isotropic displacement parameters ($Å^2 \times 10^3$) for the complex of quinuclidine betaine with *p*-hydroxybenzoic acid (1). *U*(eq) is defined as one third of the trace of the orthogonalized U_{ij} tensor.

Atom	x	y	z	U_{eq}/U_{iso}	Atom	x	y	z	U_{eq}/U_{iso}
N(1)	6632(1)	4701(1)	2710(1)	38(1)	N(11)	9209(1)	9093(1)	12903(1)	38(1)
C(2)	7408(1)	3692(1)	2203(1)	47(1)	C(12)	9600(2)	9356(2)	13830(1)	56(1)
C(3)	6651(2)	3337(2)	1575(2)	68(1)	C(13)	8395(2)	9647(2)	14768(2)	71(1)
C(4)	5274(2)	4012(2)	1758(1)	61(1)	C(14)	7171(2)	9457(2)	14544(1)	60(1)
C(5)	5433(4)	5255(2)	1243(3)	92(1)	C(15)	7355(2)	8228(2)	14404(2)	70(1)
C(6)	6293(2)	5657(1)	1760(1)	54(1)	C(16)	8514(2)	8033(1)	13390(2)	55(1)
C(7)	4658(2)	3769(3)	3029(2)	83(1)	C(17)	7023(2)	10278(2)	13450(1)	58(1)
C(8)	5358(1)	4370(2)	3556(1)	50(1)	C(18)	8271(1)	10109(1)	12496(1)	44(1)
C(9)	7402(2)	5158(1)	3251(1)	49(1)	C(19)	10449(1)	8906(1)	11976(1)	43(1)
C(10)	7722(1)	4381(1)	4316(1)	47(1)	C(20)	10364(1)	8524(1)	10962(1)	41(1)
O(1)	7770(1)	3315(1)	4491(1)	56(1)	O(6)	9267(1)	8444(1)	10879(1)	60(1)
O(2)	7949(1)	4932(1)	4904(1)	72(1)	O(7)	11451(1)	8300(1)	10291(1)	51(1)
C(21)	5471(1)	829(1)	7701(1)	41(1)	C(31)	9047(1)	6446(1)	8205(1)	37(1)
C(22)	6278(1)	−219(1)	7894(1)	48(1)	C(32)	8905(1)	5328(1)	8821(1)	45(1)
C(23)	5790(1)	−1149(1)	8703(1)	53(1)	C(33)	8757(2)	4499(1)	8336(1)	50(1)
C(24)	4485(1)	−1045(1)	9354(1)	44(1)	C(34)	8762(1)	4772(1)	7209(1)	42(1)
C(25)	3688(1)	13(1)	9204(1)	45(1)	C(35)	8948(1)	5874(1)	6573(1)	47(1)
C(26)	4174(1)	929(1)	8377(1)	46(1)	C(36)	9082(1)	6697(1)	7072(1)	46(1)
C(27)	5918(1)	1822(1)	6786(1)	44(1)	C(37)	9183(1)	7365(1)	8705(1)	42(1)
O(3)	7205(1)	1740(1)	6326(1)	55(1)	O(8)	9153(1)	7021(1)	9776(1)	62(1)
O(4)	5168(1)	2645(1)	6466(1)	66(1)	O(9)	9302(1)	8341(1)	8170(1)	64(1)
O(5)	4033(1)	−1983(1)	10127(1)	57(1)	O(10)	8601(1)	3937(1)	6769(1)	62(1)
H(2A)	7600(16)	3105(14)	2830(14)	49(4)	H(12A)	10140(20)	9980(20)	13459(19)	86(7)
H(2B)	8170(20)	3978(17)	1699(17)	66(5)	H(12B)	10150(20)	8630(20)	14125(18)	81(6)
H(3A)	6580(30)	2540(30)	1830(20)	110(9)	H(13A)	8480(30)	9220(20)	15480(20)	104(8)
H(3B)	7120(30)	3530(30)	650(30)	122(9)	H(13B)	8280(30)	10500(30)	14720(20)	117(9)
H(4)	4730(20)	3749(19)	1401(18)	79(6)	H(14)	6400(20)	9595(18)	15172(18)	77(6)
H(5A)	4590(30)	5700(30)	1390(30)	130(11)	H(15A)	6600(30)	8110(20)	14250(20)	97(8)
H(5B)	5670(30)	5450(30)	510(30)	129(11)	H(15B)	7500(20)	7660(20)	15120(20)	99(7)
H(6A)	7160(20)	5842(19)	1223(19)	81(6)	H(16A)	9140(20)	7410(20)	13595(18)	78(6)
H(6B)	5879(18)	6310(17)	2100(16)	64(5)	H(16B)	8220(20)	7940(19)	12710(19)	84(6)
H(7A)	3630(30)	3960(20)	3340(20)	101(8)	H(17A)	6260(20)	10118(18)	13243(18)	76(6)
H(7B)	4359(12)	4534(12)	2889(10)	18(3)	H(17B)	6880(20)	11040(20)	13570(19)	85(6)
H(8A)	4848(19)	5097(18)	3776(16)	69(5)	H(18A)	8088(17)	9928(15)	11863(15)	59(5)
H(8B)	5587(19)	3774(17)	4160(17)	66(5)	H(18B)	8768(19)	10751(17)	12244(16)	66(5)
H(9A)	6870(20)	5847(18)	3443(16)	68(5)	H(19A)	10788(16)	9655(15)	11713(14)	53(4)
H(9B)	8270(20)	5299(16)	2674(17)	66(5)	H(19B)	11049(17)	8334(15)	12314(14)	56(5)
H(22)	7178(18)	−290(15)	7469(15)	59(5)	H(32)	8924(17)	5130(15)	9605(16)	57(5)
H(23)	6329(19)	−1883(18)	8829(16)	69(5)	H(33)	8677(19)	3730(18)	8772(17)	71(5)
H(25)	2802(18)	69(15)	9670(15)	58(5)	H(35)	8982(18)	6006(16)	5800(16)	63(5)
H(26)	3601(17)	1669(15)	8278(14)	55(4)	H(36)	9220(18)	7472(17)	6627(16)	66(5)
H(3)	7390(20)	2380(20)	5680(20)	92(7)	H(8)	9290(20)	7660(20)	10082(19)	88(7)
H(5)	3130(20)	−1860(20)	10304(19)	88(7)	H(10)	8430(20)	4290(20)	6060(20)	98(8)

conformation. The average magnitudes of the angles are $-9 \pm 4.3°$ for N(1)–C–C–C(4) and $5.9 \pm 0.3°$ for N(11)–C–C–C(14) (Table 3). However, the ethylene N(1)–C(8)–C(7)–C(4) carbons have the largest thermal ellipsoids of all atoms in this structure (Fig. 2), which clearly indicates that these atoms vibrate strongly and perpendicular to the average N(1)–C–C–C(4) planes. This is connected with the low conformational stability of the ethylene bridges, which have low potential energy (planar conformation metastable) for the conversion to the opposite propeller turns. The strong vibrations of the N(1)–C–C–C(4) ethylene carbons are the likely reason for the differences in these torsion-angle magnitudes. The opposite signs of the torsion angles in the two QNB moieties indicate the opposite sense of the propeller turns. The propeller conformation of quinuclidine moiety was observed in quinuclidine betaine hydrate [15], *N*-(carbethoxymethyl)quinuclidinium chloride dihydrate [26] and in the complex of quinuclidine betaine with tartaric acid [27]. Analogous conformational features were reported for 1,4-diazabicyclo[2.2.2]octane, its H-bonded complexes and derivatives [28–36].

The conformation of the HBA molecule can be described by the dihedral angle between the plane of the aromatic rings and the carboxyl group, and they are 14.5(2)° and 1.3(2)°, in two symmetry-independent molecules, respectively (Figs. 3 and 4).

The O–H···O bonded zigzag chains interact with their neighboring chains mainly via weak C–H···O and van der Waals contacts. The most pronounced C–H···O contacts involve carbonyl oxygens of the carbonyl groups: C(6)–H(6B)···O(4)^b of 3.279(3) Å and C(18)–H(18B)···O(9)^c of 3.318(3) Å [symmetry codes: $^b1-x, 1-y, 1-z$; $^c2-x, 2-y, 2-z$] (Table 4). It is characteristic that for both the carboxyl groups the shortest C–H···O contacts are formed to the α-methylene hydrogens of quinuclidinium moieties (for the atomic labeling see Fig. 1), which indicates the role of the electrostatic attraction in these interactions [37–50].

3.2. B3LYP/6-31G(d,p) calculations

The structures of the 2:2 complex of quinuclidine betaine with HBA (**2**) and two 1:1 complexes of QNB·HBA (**3** and **4**) optimized at the B3LYP/6-31G(d,p) level of theory are shown in Fig. 5. Similarly as in the crystals, the optimized structure **2** is built of two independent QNB·HBA units (Table 3). The molecules are linked by the O(3)–H···O(1)–C(10), C(10)–O(2)···H–O(10) and C(37)–O(8)–H···O(6)–C(20) hydrogen bonds of 2.616, 2.713 and 2.586 Å, respectively (Table 4). All these calculated O···O distances are longer than those observed in the crystal. The propeller conformations in both quinuclidinium fused-rings systems are also observed. The

Table 3
Experimental (**1**) and calculated (**2**) by the B3LYP/6-31G(d,p) level of theory bond lengths (Å), bond and selected angles (°) for the complex of quinuclidine betaine with *p*-hydroxybenzoic acid.

Parameters	X-ray **1**	B3LYP **2**	Parameters	X-ray **1**	B3LYP **2**
Bond lengths					
N(1)–C(2)	1.507(2)	1.527	N(11)–C(12)	1.509(2)	1.513
C(2)–C(3)	1.505(2)	1.542	C(12)–C(13)	1.516(2)	1.546
C(3)–C(4)	1.518(3)	1.540	C(13)–C(14)	1.518(3)	1.541
C(4)–C(5)	1.498(3)	1.540	C(14)–C(15)	1.515(3)	1.540
C(5)–C(6)	1.519(3)	1.545	C(15)–C(16)	1.521(2)	1.542
N(1)–C(6)	1.517(2)	1.515	N(11)–C(16)	1.515(2)	1.526
C(4)–C(7)	1.520(3)	1.539	C(14)–C(17)	1.517(2)	1.538
C(7)–C(8)	1.547(3)	1.542	C(17)–C(18)	1.523(2)	1.542
N(1)–C(8)	1.511(2)	1.527	N(11)–C(18)	1.509(2)	1.525
N(1)–C(9)	1.503(2)	1.516	N(11)–C(19)	1.503(2)	1.521
C(9)–C(10)	1.529(2)	1.560	C(19)–C(20)	1.527(2)	1.574
C(10)–O(1)	1.246(2)	1.257	C(20)–O(6)	1.252(2)	1.270
C(10)–O(2)	1.240(2)	1.245	C(20)–O(7)	1.241(2)	1.229
C(21)–C(22)	1.391(2)	1.404	C(31)–C(32)	1.387(2)	1.406
C(22)–C(23)	1.379(2)	1.388	C(32)–C(33)	1.379(2)	1.387
C(23)–C(24)	1.391(2)	1.401	C(33)–C(34)	1.390(2)	1.408
C(24)–O(5)	1.355(2)	1.363	C(34)–O(10)	1.350(2)	1.344
C(24)–C(25)	1.389(2)	1.401	C(34)–C(35)	1.384(2)	1.409
C(25)–C(26)	1.377(2)	1.390	C(35)–C(36)	1.378(2)	1.388
C(21)–C(26)	1.394(2)	1.400	C(31)–C(36)	1.389(2)	1.403
C(21)–C(27)	1.478(2)	1.487	C(31)–C(37)	1.483(2)	1.483
C(27)–O(3)	1.321(2)	1.325	C(37)–O(8)	1.313(2)	1.326
C(27)–O(4)	1.213(2)	1.233	C(37)–O(9)	1.209(2)	1.237
Bond angles					
N(1)–C(2)–C(3)	110.63(12)	109.58	N(11)–C(12)–C(13)	110.86(13)	110.21
C(2)–C(3)–C(4)	110.20(13)	109.18	C(12)–C(13)–C(14)	109.63(14)	108.83
C(3)–C(4)–C(5)	106.68(19)	108.78	C(13)–C(14)–C(15)	108.66(16)	108.84
C(4)–C(5)–C(6)	110.70(14)	108.84	C(14)–C(15)–C(16)	110.43(13)	109.12
N(1)–C(6)–C(5)	109.78(13)	110.22	N(11)–C(16)–C(15)	109.84(13)	109.64
C(2)–N(1)–C(6)	107.48(10)	108.21	C(12)–N(11)–C(16)	108.34(12)	108.21
C(3)–C(4)–C(7)	105.75(16)	108.34	C(13)–C(14)–C(17)	108.42(16)	108.52
C(5)–C(4)–C(7)	113.6(2)	108.50	C(15)–C(14)–C(17)	108.73(15)	108.23
C(4)–C(7)–C(8)	108.41(15)	108.94	C(14)–C(17)–C(18)	109.97(12)	108.87
N(1)–C(8)–C(7)	109.65(12)	110.07	N(11)–C(18)–C(17)	110.23(11)	110.16
C(2)–N(1)–C(8)	110.19(11)	109.08	C(12)–N(11)–C(18)	108.34(11)	108.60
C(6)–N(1)–C(8)	108.00(11)	108.58	C(16)–N(11)–C(18)	109.31(11)	109.18
C(9)–N(1)–C(2)	112.45(11)	111.53	C(19)–N(11)–C(12)	107.17(10)	109.87
C(9)–N(1)–C(6)	108.15(11)	109.16	C(19)–N(11)–C(16)	112.28(10)	111.18
C(9)–N(1)–C(8)	110.40(10)	110.20	C(19)–N(11)–C(18)	111.26(10)	109.74
N(1)–C(9)–C(10)	117.16(11)	116.39	N(11)–C(19)–C(20)	118.62(10)	116.51
O(1)–C(10)–C(9)	119.95(12)	116.90	O(6)–C(20)–C(19)	120.06(11)	114.94
O(2)–C(10)–C(9)	112.46(14)	112.62	O(7)–C(20)–C(19)	113.68(11)	113.52
O(1)–C(10)–O(2)	127.56(14)	130.44	O(6)–C(20)–O(7)	126.25(12)	131.48
C(21)–C(22)–C(23)	120.79(13)	120.69	C(31)–C(32)–C(33)	121.08(12)	120.76
C(22)–C(23)–C(24)	120.24(13)	119.73	C(32)–C(33)–C(34)	120.07(12)	120.41
C(23)–C(24)–C(25)	119.41(13)	120.12	C(33)–C(34)–C(35)	119.42(12)	119.15
C(24)–C(25)–C(26)	119.91(12)	119.69	C(34)–C(35)–C(36)	119.85(12)	119.84
C(25)–C(26)–C(21)	121.21(13)	120.75	C(35)–C(36)–C(31)	121.43(12)	121.29
C(22)–C(21)–C(26)	118.33(13)	119.04	C(32)–C(31)–C(36)	118.09(11)	118.56
C(22)–C(21)–C(27)	122.80(12)	122.04	C(32)–C(31)–C(37)	122.51(11)	122.18
C(26)–C(21)–C(27)	118.83(12)	118.93	C(36)–C(31)–C(37)	119.39(11)	119.26
O(3)–C(27)–C(21)	114.86(11)	113.37	O(8)–C(37)–C(31)	113.83(11)	113.83
O(4)–C(27)–C(21)	123.02(12)	122.41	O(9)–C(37)–C(31)	122.66(13)	122.42
O(4)–C(27)–O(3)	122.11(13)	124.22	O(9)–C(37)–O(8)	123.51(12)	123.74
O(5)–C(24)–C(23)	118.65(13)	117.35	O(10)–C(34)–C(33)	118.20(13)	117.80
O(5)–C(24)–C(25)	121.93(12)	122.54	O(10)–C(34)–C(35)	122.37(13)	123.05
Torsion angles					
N(1)–C(2)–C(3)–C(4)	−6.5(2)	16.01	N(11)–C(12)–C(13)–C(14)	6.2(2)	−14.07
C(2)–C(3)–C(4)–C(5)	63.9(2)	49.22	C(12)–C(13)–C(14)–C(15)	55.3(2)	66.69
C(3)–C(4)–C(5)–C(6)	−57.0(3)	−66.91	C(13)–C(14)–C(15)–C(16)	−62.3(2)	−49.14
C(4)–C(5)–C(6)–N(1)	−4.8(3)	14.35	C(14)–C(15)–C(16)–N(11)	5.5(2)	−16.03
C(2)–N(1)–C(6)–C(5)	62.2(2)	50.83	C(12)–N(11)–C(16)–C(15)	55.7(2)	69.02
C(6)–N(1)–C(2)–C(3)	−55.6(2)	−68.86	C(16)–N(11)–C(12)–C(13)	−62.9(2)	−51.04
C(2)–C(3)–C(4)–C(7)	−57.3(2)	−68.55	C(12)–C(13)–C(14)–C(17)	−62.7(2)	−50.95
C(7)–C(4)–C(5)–C(6)	59.1(3)	50.75	C(17)–C(14)–C(15)–C(16)	55.5(2)	68.65
C(4)–C(7)–C(8)–N(1)	−15.6(2)	14.56	C(14)–C(17)–C(18)–N(11)	6.1(2)	−14.19
C(3)–C(4)–C(7)–C(8)	69.7(2)	50.44	C(13)–C(14)–C(17)–C(18)	55.6(2)	67.26
C(5)–C(4)–C(7)–C(8)	−46.9(2)	−67.51	C(15)–C(14)–C(17)–C(18)	−62.4(2)	67.26
C(8)–N(1)–C(2)–C(3)	61.9(2)	49.10	C(18)–N(11)–C(12)–C(13)	55.6(2)	67.36
C(8)–N(1)–C(6)–C(5)	−56.7(2)	−67.45	C(18)–N(11)–C(16)–C(15)	−62.2(2)	−49.01
C(2)–N(1)–C(8)–C(7)	−48.5(2)	−67.37	C(12)–N(11)–C(18)–C(17)	−62.6(2)	−50.71

(*continued on next page*)

Table 3 (*continued*)

Parameters	X-ray **1**	B3LYP **2**	Parameters	X-ray **1**	B3LYP **2**
C(6)–N(1)–C(8)–C(7)	68.6(2)	50.36	C(16)–N(11)–C(18)–C(17)	55.3(2)	67.08
C(9)–N(1)–C(2)–C(3)	−174.5(1)	171.06	C(19)–N(11)–C(12)–C(13)	175.7(2)	−172.60
C(9)–N(1)–C(6)–C(5)	−176.2(2)	172.38	C(19)–N(11)–C(16)–C(15)	173.8(1)	−170.23
C(9)–N(1)–C(8)–C(7)	−173.4(2)	169.87	C(19)–N(11)–C(18)–C(17)	179.9(1)	−170.83
C(2)–N(1)–C(9)–C(10)	−67.9(2)	−68.26	C(12)–N(11)–C(19)–C(20)	174.9(1)	−171.59
C(6)–N(1)–C(9)–C(10)	173.6(1)	172.21	C(16)–N(11)–C(19)–C(20)	56.2(2)	68.64
C(8)–N(1)–C(9)–C(10)	55.6(2)	53.05	C(18)–N(11)–C(19)–C(20)	−66.8(2)	−52.25
N(1)–C(9)–C(10)–O(1)	24.6(2)	27.12	N(11)–C(19)–C(20)–O(6)	4.6(2)	−29.49
N(1)–C(9)–C(10)–O(2)	−157.5(1)	−155.02	N(11)–C(19)–C(20)–O(7)	−174.3(1)	152.95
C(21)–C(22)–C(23)–C(24)	−1.2(2)	0.08	C(31)–C(32)–C(33)–C(34)	0.7(2)	0.08
C(22)–C(23)–C(24)–C(25)	−1.8(2)	−0.04	C(32)–C(33)–C(34)–C(35)	1.5(2)	−0.01
C(23)–C(24)–C(25)–C(26)	3.3(2)	−0.05	C(33)–C(34)–C(35)–C(36)	−2.2(2)	−0.08
C(24)–C(25)–C(26)–C(21)	−1.8(2)	0.08	C(34)–C(35)–C(36)–C(31)	0.6(2)	0.11
C(26)–C(21)–C(22)–C(23)	2.7(2)	−0.05	C(36)–C(31)–C(32)–C(33)	−2.2(2)	−0.06
C(22)–C(21)–C(26)–C(25)	−1.2(2)	−0.03	C(32)–C(31)–C(36)–C(35)	1.6(2)	−0.04
C(22)–C(23)–C(24)–O(5)	178.9(1)	179.98	C(32)–C(33)–C(34)–O(10)	−179.4(1)	−179.90
C(26)–C(25)–C(24)–O(5)	−177.4(1)	179.94	C(36)–C(35)–C(34)–O(10)	178.8(1)	179.80
C(27)–C(21)–C(22)–C(23)	−175.1(1)	179.90	C(37)–C(31)–C(32)–C(33)	178.9(1)	179.69
C(27)–C(21)–C(26)–C(25)	176.7(1)	−179.98	C(37)–C(31)–C(36)–C(35)	−179.5(1)	−179.79
C(22)–C(21)–C(27)–O(3)	−14.3(2)	0.37	C(32)–C(31)–C(37)–O(8)	−0.2(2)	2.01
C(26)–C(21)–C(27)–O(3)	168.0(1)	−179.68	C(36)–C(31)–C(37)–O(8)	−179.1(1)	−178.25
C(22)–C(21)–C(27)–O(4)	164.8(1)	−179.37	C(32)–C(31)–C(37)–O(9)	−179.7(1)	−178.19
C(26)–C(21)–C(27)–O(4)	−12.9(2)	0.58	C(36)–C(31)–C(37)–O(9)	1.8(2)	1.55

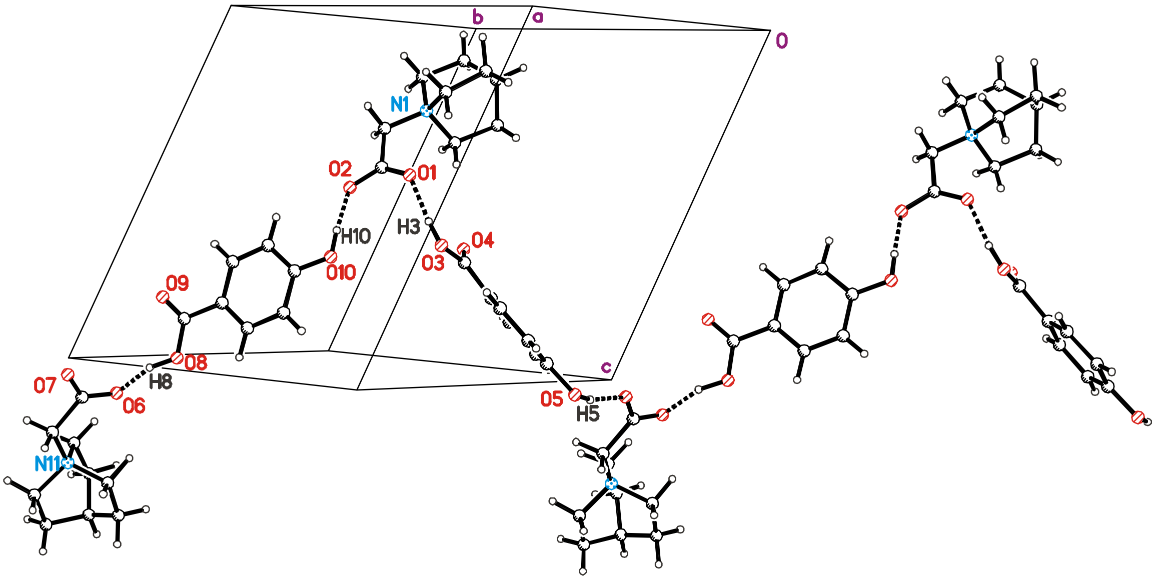

Fig. 3. The hydrogen-bonded chain of the molecules of the complex of quinuclidine betaine with *p*-hydroxybenzoic acid running along the crystal direction [1 1 0] (cf. Fig. 2). The aggregate can be perceived in 3 dimensions as an autostereogram [64].

Table 4
Experimental and calculated, at the B3LYP/6-31G(d,p) approach, hydrogen bonds dimensions, for the complex of quinuclidine betaine with *p*-hydroxybenzoic acid (Å and °).

No.	D–H···A	*d*(D–H)	*d*(H···A)	*d*(D···A)	<(DHA)
	X-ray				
1	O(3)–H(3)···O(1)	0.93(2)	1.668(21)	2.591(2)	172(3)
	O(10)–H(10)···O(2)	0.95(3)	1.664(24)	2.609(2)	174(3)
	O(8)–H(8)···O(6)	1.04(2)	1.540(23)	2.556(2)	163(3)
	O(5)–H(5)···O(7)^{a}	0.92(2)	1.794(22)	2.687(2)	165 (3)
	C(6)–H(6)···O(4)^{b}	0.96(3)	2.37(3)	3.279(3)	158(2)
	C(18)–H(18)···O(9)^{c}	0.98(3)	2.40(3)	3.318(3)	155(3)
	B3LYP/6-31G(d,p)				
2	O(3)–H(3)···O(1)	1.003	1.619	2.616	172.43
	O(10)–H(10)···O(2)	0.990	1.725	2.713	175.89
	O(8)–H(8)···O(6)	1.011	1.582	2.586	171.80
3	O(3)–H(3)···O(1)	1.026	1.519	2.539	172.35
4	O(10)–H(10)···O(2)	0.998	1.669	2.664	174.16

Symmetry code: $^{a}x-1, y-1, z$; $^{b}1-x, 1-y, 1-x$; $^{c}2-x, 2-y, 2-z$.

magnitude of the N–CH$_2$–CH$_2$–C(4) torsion angles is similar in both rings, and are ca. 14° (Table 3). In the optimized structure **3** QNB is linked with HBA by the COO···HOOC hydrogen bond of 2.539 Å, while in the structure **4** the hydroxyl group of HBA interacts with the carboxylate group of QNB and the O···O distance is 2.664 Å.

The calculated energies and dipole moments for **2**, **3**, **4**, QNB and HBA determined by the B3LYP/6-31G(d,p) level of theory are listed in Table 5. Morokuma and coworkers [51–53] defined energy stabilization as a difference between the energy of the global system and the total energy of the separate partners: $\Delta E = E_{\mathrm{COMPLEX}} - E_{\mathrm{COMPONENTS}}$. The estimated binding energy (ΔE) of the QNB molecule by HBA are listed in Table 5, and it increases in order **2** > **3** > **4**, as expected.

3.3. Infrared spectra

The solid-state FTIR spectrum of the crystalline QNB·HBA complex is shown in Fig. 6. According to the crystal structure (Table 4)

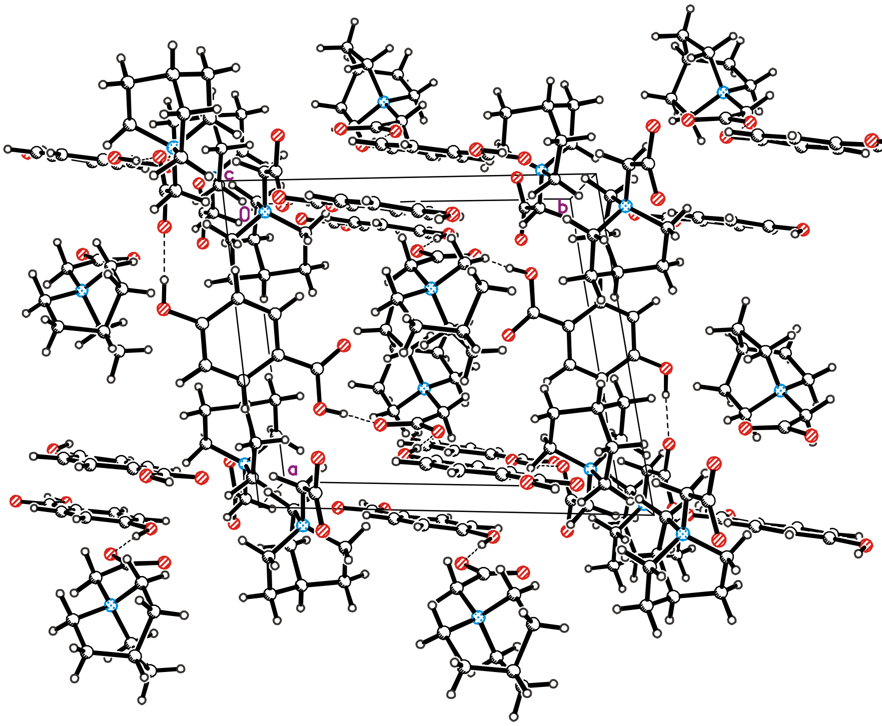

Fig. 4. The molecular arrangement of H-bonded aggregates in the complex of quinuclidine betaine with *p*-hydroxybenzoic acid viewed down the [0 0 1] direction.

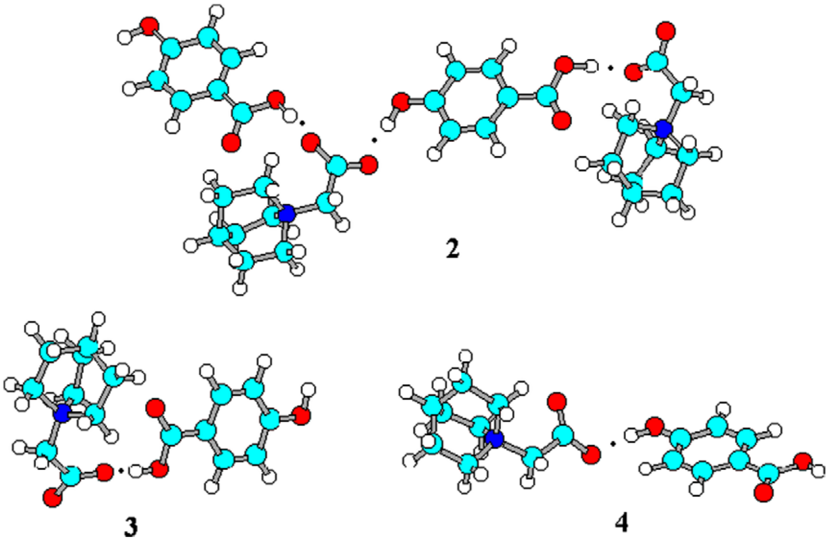

Fig. 5. The structure of complexes of quinuclidine betaine with *p*-hydroxybenzoic acid optimized at the B3LYP/6-31G(d.p) level of theory at the ratio 2:2 (**2**) and 1:1 (**3** and **4**).

there are two moderate O–H···O hydrogen bonds in the complex investigated. As a consequence, the νOH absorption appears in the 3200–1800 cm^{-1} region. The contour of this absorption is known as the ABC bands, which are observed in the spectra of hydrogen-bonded carboxylic acid. The A (~2800 cm^{-1}), B (~2500 cm^{-1}) and C (~1900 cm^{-1}) bands arise from the Fermi resonance of the ν_{OH} with $2\delta_{OH}$ and $2\gamma_{OH}$ [54–56]. This trio of bands is observed in the spectrum of the complex investigated (Fig. 6). Deuterium substitution affects all three bands. Band A and B disappear and new bands appear at 2300 and 2000 cm^{-1}, while band C from 1900 cm^{-1} shifts to 1635 cm^{-1} and overlaps the carbonyl band.

The bands at 1680 and 1600 cm^{-1} are attributed to the νC=O and ν_{as}COO vibrations of HBA and QNB moieties, respectively. The second-derivative spectrum [57,58] shows several minima in the range of 1750–1550 cm^{-1}, which confirm the presence of two non-equivalent QNB·HBA complexes (Fig. 7). The strong band

Table 5
Calculated energies (*E*, HF, a.u.), dipole moments (μ, *D*) and binding energies (ΔE, kcal/mol) at B3LYP/6-31G(d,p) approach for the complexes of quinuclidine betaine (QNB) with *p*-hydroxybenzoic acid (HBA).

Compound[a]	*E*	ΔE	μ
2	–2106.5579485	–34.98	22.37
3	–1053.2676116	–20.73	10.81
4	–1053.2652737	–19.23	17.68
QNB	–557.1767069		11.57
HBA	–496.0578548		1.85

[a] See Fig. 5.

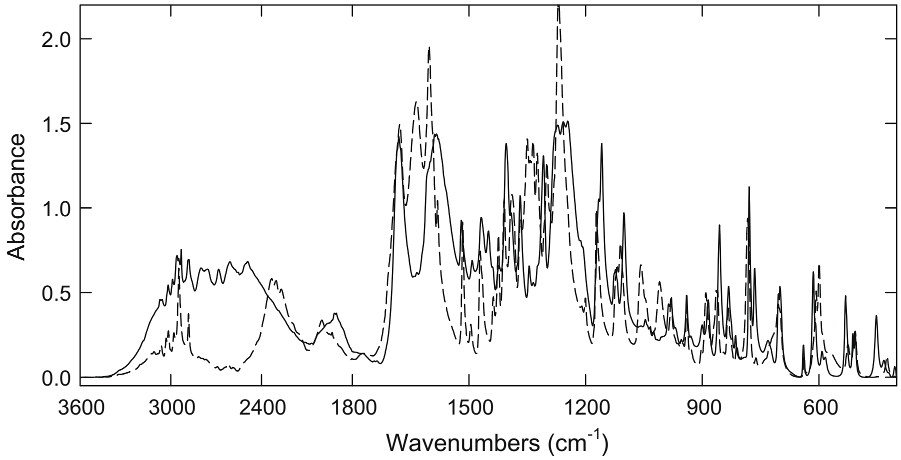

Fig. 6. The solid-state FTIR spectrum in Nujol and Fluorolube emulsions of the quinuclidine betaine – *p*-hydroxybenzoic acid complex; dashed line of the spectrum of the deuterated sample.

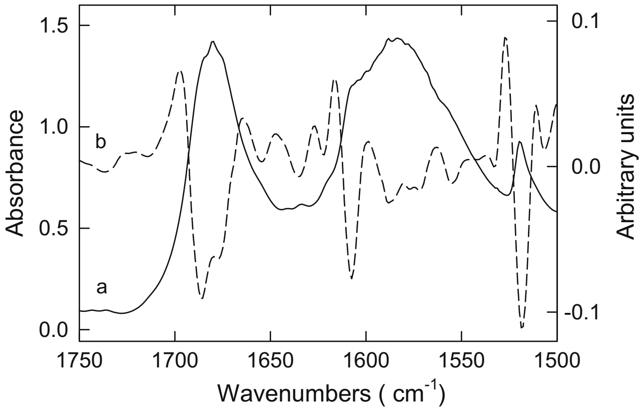

Fig. 7. Infrared spectra of the complex of quinuclidine betaine with *p*-hydroxybenzoic acid: (a) solid line the FTIR spectrum in Fluorolube emulsions and (b) dashed line the second-derivative FTIR spectrum in the 1750–1500 cm^{-1} region.

at 1270 cm^{-1} is assigned to the ν_sCOO mode (Fig. 6). The bands at 1584, 1470 and 1250 cm^{-1} are due to the bending in-plane OH modes (δOH) of hydrogen bonds, which are shifted to 1350 and 1010 cm^{-1} in the spectrum of the deuterated sample. The bands at 779, 614 and 451 cm^{-1} are assigned to the bending out-of-plane OH modes (γOH), however, only one band assigned to the γOD is observed at 599 cm^{-1} in the spectrum of deuterated sample, the others appear below 400 cm^{-1} and are not detected.

3.4. NMR studies

Both the ^{1}H and ^{13}C NMR spectra (Fig. 8) in DMSO-d_6 show that the investigated complex exists as 1:1 species. The proton and carbon-13 chemical shifts are listed in Table 6. The carbon atoms attached to the quaternary nitrogen atom are denoted as α, the others as β and γ (Fig. 1). The ^{1}H NMR spectrum is simple, similar to those of other quinuclidinium betaine derivatives [15,26,27,59].

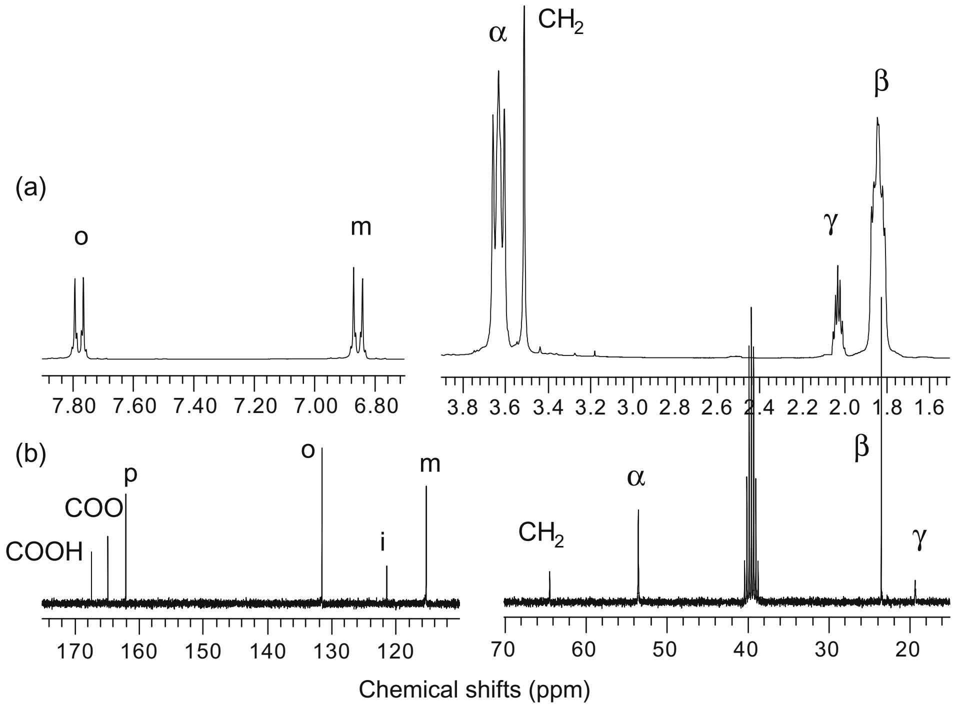

Fig. 8. ^{1}H (a) and ^{13}C (b) NMR spectra of the complex of quinuclidine betaine with *p*-hydroxybenzoic acid in DMSO-d_6.

Table 6
Experimental (δ_{exp}, in DMSO-d_6) and predicted (δ_{pred}, in vacuum and DMSO) proton and carbon-13 chemical shifts (ppm), and calculated magnetic isotropic shielding tensors (σ) by the GIAO/B3LYP/6-31G(d,p) calculations for complex **3** of quinuclidine betaine with *p*-hydroxybenzoic acid.

Atom[a]	δ_{exp} DMSO-d_6	δ_{pred} DMSO	σ DMSO	δ_{pred} Vacuum	σ Vacuum
^1H					
H-α	3.63	3.68	27.8833 ± 1.1792	3.97	27.7472 ± 2.0648
H-β	1.90	1.87	29.7131 ± 0.0553	2.00	29.7482 ± 0.4709
H-γ	2.03	2.17	29.4041	2.04	29.7136
N^+–CH_2	3.51	3.09	28.4737 ± 0.0868	2.84	28.8985 ± 0.0999
H-*ortho*	7.78	2.04	23.4701 ± 0.0255	8.13	23.5058 ± 0.1186
H-*meta*	6.86	6.83	24.6920 ± 0.0387	6.51	25.1603 ± 0.2710
a[b]			31.2492		31.2115
b[b]			−0.9888		−0.9818
r			0.9913		0.9778
^{13}C					
C-α	53.44	54.50	136.0652 ± 2.7109	53.94	136.1032 ± 2.2096
C-β	23.47	22.77	165.7150 ± 0.1320	22.12	165.3555 ± 0.9098
C-γ	19.29	19.67	168.6166	20.02	167.2874
N^+–CH_2	64.37	64.39	126.8244	66.42	124.6234
COO	164.81	164.81	32.9946	156.93	41.4046
C-*ortho*	131.45	131.50	64.1156 ± 0.3257	132.51	63.8646 ± 0.5491
C-*meta*	115.21	112.42	81.9524 ± 0.0774	111.20	83.4499 ± 1.1343
C-*para*	162.00	160.75	36.7882	159.48	39.0593
C-*ipso*	121.34	122.52	72.5145	126.03	69.8160
COOH	167.33	168.69	29.3699	170.34	29.0775
a[b]			200.1221		201.9644
b[b]			−1.0702		−1.0876
r			0.9996		0.9987

[a] For atoms numbering see Fig. 1.
[b] Coefficients for the equation: $\delta_{exp} = a + b\sigma$.

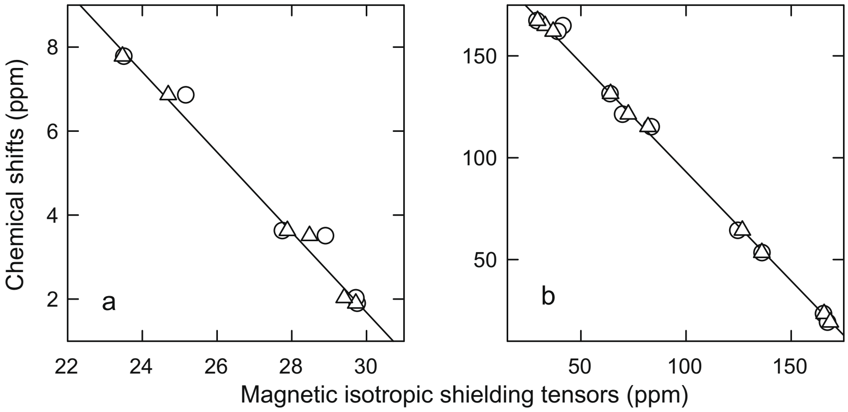

Fig. 9. Plots of the experimental ^1H (a) and ^{13}C (b) chemical shifts (in DMSO-d_6) versus the magnetic isotropic shielding tensors from the GIAO/B3LYP/6-31G(d,p) calculations for the complex of quinuclidine betaine with *p*-hydroxybenzoic acid; ○ in vacuum, Δ in DMSO solution (the correlation line is given for values in the DMSO solution).

The average values of the magnetic isotropic shielding tensors (σ), calculated by the GIAO/B3LYP/6-31G(p,d) approach for the 1:1 complex of QNB·HBA (**3**) in vacuum and in the DMSO solution, are given in Table 6. The linear relations between the experimental chemical shifts and the magnetic isotropic shielding tensors are described by the following equation: $\delta_{exp} = a + b\sigma$ [60–62] and shown in Fig. 9. The correlation coefficients (*r*) show that these relationships are better for carbon than for protons (Table 6). The protons are located on the peripheries of the molecules and thus are supposed to be more susceptible to intermolecular (solvent–solute) effects than carbons [63]. The *a* and *b* coefficients are used to calculate the predicted ^1H and ^{13}C chemical shifts (δ_{pred}) (Table 6). The agreement between the experimental and predicted ^1H and ^{13}C chemical shifts is better in the DMSO solution than in vacuum.

4. Conclusions

Two symmetry-independent molecules of the complex of quinuclidine betaine (QNB) with *p*-hydroxybenzoic acid (HBA) are linked into chain, by a sequence of O–H···O hydrogen bonds. Both carboxylate oxygen atoms of each QNB molecule are involved in the hydrogen bonds with COOH (2.591(2), 2.556(2) Å) and OH (2.609(2), 2.687(2) Å) groups of two neighboring HBA molecules. These medium-strong hydrogen bonds result a trio ABC bands in the 2800–1900 cm^{-1} region in the IR spectra characteristic of the hydrogen-bonded carboxylic acids. The calculated magnetic isotropic shielding tensors (σ) correlate linearly with the experimental ^1H and ^{13}C chemical shifts ($\delta_{exp} = a + b\sigma$), which confirms correct assignments of the chemical shifts. The optimized structure of the 1:1 complex of QNB···HOOC–C_6H_4OH (**3**) is by 1.47 kcal/mol more stable than that of the complex QNB···HO–C_6H_4COOH (**4**). The binding energies, ΔE, for the optimized structure **2**, **3** and **4** confirm that the 2:2 complex of QNB with HBA is a more stable then the 1:1 complexes **3** and **4**.

Acknowledgement

DFT calculations were performed at the Poznań Supercomputing and Networking Centre.

References

[1] K. Fukuyama, K. Ohkura, S. Kashino, M. Haisa, Bull. Chem. Soc. 46 (1973) 804.
[2] M. Colapietro, A. Domenicano, C. Marciante, Acta Cryst. B35 (1979) 2177.
[3] E.A. Heath, P. Singh, Y. Ebisuzaki, Acta Cryst. C48 (1992) 1960.
[4] T.-J. Hsieh, C.-C. Su, C.-Y. Chen, C.-H. Liou, L.H. Lu, J. Mol. Struct. 741 (2005) 193.
[5] J. Hermans, S.J. Leach, H.A. Scherage, J. Am. Chem. Soc. 85 (1963) 1390.
[6] C.A. Hollingsworth, P.G. Seybold, C.M. Hadad, Int. J. Quantum Chem. 90 (2002) 1396.
[7] Z. Dega-Szafran, G. Dutkiewicz, Z. Kosturkiewicz, M. Przedwojska, M. Szafran, J. Mol. Struct. 649 (2003) 257.
[8] Z. Dega-Szafran, G. Dutkiewicz, Z. Kosturkiewicz, M. Szafran, J. Mol. Struct. 875 (2008) 346.
[9] Z. Dega-Szafran, A. Katrusiak, M. Szafran, J. Mol. Struct. 785 (2006) 160.
[10] Z. Dega-Szafran, A. Katrusiak, M. Szafran, J. Mol. Struct. 797 (2006) 82.
[11] Z. Dega-Szafran, G. Dutkiewicz, Z. Kosturkiewicz, M. Szafran, J. Mol. Struct. 844–845 (2007) 38.
[12] Z. Dega-Szafran, M. Jaskólski, M. Szafran, Polish J. Chem. 81 (2007) 931.
[13] E. Bartoszak-Adamska, Z. Dega-Szafran, M. Krociak, M. Jaskólski, M. Szafran, J. Mol. Struct. 920 (2009) 68.
[14] Z. Dega-Szafran, G. Dutkiewicz, Z. Kosturkiewicz, M. Szafran, J. Mol. Struct. 923 (2009) 72.
[15] Z. Dega-Szafran, A. Katrusiak, M. Szafran, J. Mol. Struct. 921 (2009) 295.
[16] KUMA KM4 CCD Software, version 161, Kuma Diffraction, Wroclaw, Poland, 1999.
[17] CrysAlis 162, Kuma Diffraction, Wroclaw, Poland, 1999.
[18] G.M. Sheldrick, SHELXS-97, Program for Solution of the Crystal Structures, University of Göttingen, Germany, 1997.
[19] G.M. Sheldrick, SHELXL-97, Program for Crystal Structure Refinement, University of Göttingen, Germany, 1997.
[20] M.J. Frisch, G.W. Trucks, H.B. Schlegel, G.E. Scuseria, M.A. Robb, J.R. Cheeseman, J.A. Montgomery Jr., T. Vreven, K.N. Kudin, J.C. Burant, J.M. Millam, S.S. Iyengar, J. Tomasi, V. Barone, B. Mennucci, M. Cossi, G. Scalmani, N. Rega, G.A. Petersson, H. Nakatsuji, M. Hada, M. Ehara, K. Toyota, R. Fukuda, J. Hasegawa, M. Ishida, T. Nakajima, Y. Honda, O. Kitao, H. Nakai, M. Klene, X. Li, J.E. Knox, H.P. Hratchian, J.B. Cross, V. Bakken, C. Adamo, J. Jaramillo, R. Gomperts, R.E. Stratmann, O. Yazyev, A.J. Austin, R. Cammi, C. Pomelli, J.W. Ochterski, P.Y. Ayala, K. Morokuma, G.A. Voth, P. Salvador, J.J. Dannenberg, V.G. Zakrzewski, S. Dapprich, A.D. Daniels, M.C. Strain, O. Farkas, D.K. Malick, A.D. Rabuck, K. Raghavachari, J.B. Foresman, J.V. Ortiz, Q. Cui, A.G. Baboul, S. Clifford, J. Cioslowski, B.B. Stefanov, G. Liu, A. Liashenko, P. Piskorz, I. Komaromi, R.L. Martin, D.J. Fox, T. Keith, M.A. Al-Laham, C.Y. Peng, A. Nanayakkara, M. Challacombe, P.M.W. Gill, B. Johnson, W. Chen, M.W. Wong, C. Gonzalez, J.A. Pople, GAUSSIAN 03, Revision D.02, Gaussian, Inc., Wallingford CT, 2004.
[21] A.D. Becke, J. Chem. Phys. 98 (1993) 5648.
[22] A.D. Becke, J. Chem. Phys. 107 (1997) 8554.
[23] C. Lee, W. Yang, G.R. Parr, Phys. Rev. B 37 (1988) 785.
[24] W.J. Hehre, L. Random, P.V.R. Schleyer, J.A. Pople, Ab Initio Molecular Orbital Theory, Wiley, New York, 1986.
[25] V. Barone, M. Cossi, J. Phys. Chem. 102A (1998) 1995.
[26] Z. Dega-Szafran, A. Katrusiak, M. Szafran, Polish J. Chem. 83 (2009) 723.
[27] Z. Dega-Szafran, A. Katrusiak, M. Szafran, J. Mol. Struct. 936 (2009) 9.
[28] O.J. Żogał, Z. Galewski, E. Grech, Z. Malarski, Mol. Phys. 56 (1985) 673.
[29] A. Katrusiak, M. Szafranski, Phys. Rev. Lett. 82 (1999) 576.
[30] A. Katrusiak, M. Ratajczak-Sitarz, E. Grech, J. Mol. Struct. 474 (1999) 135.
[31] M. Szafranski, A. Katrusiak, Chem. Phys. Lett. 318 (2000) 427.
[32] M. Szafranski, A. Katrusiak, G. McIntyre, Phys. Rev. Lett. 89 (2002) 215507-1.
[33] M. Szafranski, A. Katrusiak, J. Phys. Chem. B 108 (2004) 15709.
[34] A. Budzianowski, A. Katrusiak, M. Szafranski, J. Phys. Chem. B 112 (2008) 16619.
[35] M. Szafranski, A. Katrusiak, J. Phys. Chem. B 112 (2008) 6779.
[36] P. Barczyński, Z. Dega-Szafran, A. Katrusiak, W. Perdoch, M. Szafran, J. Mol. Struct. 938 (2009) 283.
[37] A. Katrusiak, M. Szafranski, J. Am. Chem. Soc. 128 (2006) 15775.
[38] K. Dziubek, M. Podsiadlo, A. Katrusiak, J. Am. Chem. Soc. 129 (2007) 12620.
[39] K.F. Dziubek, A. Katrusiak, J. Phys. Chem. B 112 (2008) 12001.
[40] M. Bujak, M. Podsiadlo, A. Katrusiak, Chem. Commun. (2008) 4439.
[41] M. Podsiadlo, A. Katrusiak, CrystEngComm 10 (2008) 1436.
[42] A. Olejniczak, A. Katrusiak, A. Vij, J. Fluor. Chem. 129 (2008) 1090.
[43] A. Olejniczak, A. Katrusiak, P. Metrangolo, G. Resnati, J. Fluor. Chem. 130 (2009) 248.
[44] R. Gajda, A. Katrusiak, J. Phys. Chem. B 113 (2009) 2436.
[45] A. Olejniczak, A. Katrusiak, A. Vij, CrystEngComm 11 (2009) 1073.
[46] M. Podsiadlo, A. Katrusiak, CrystEngComm 11 (2009) 1951.
[47] A. Olejniczak, A. Katrusiak, A. Vij, CrystEngComm 11 (2009) 1240.
[48] A. Olejniczak, K. Ostrowska, A. Katrusiak, J. Phys. Chem. C 113 (2009) 15761.
[49] K. Dziubek, M. Podsiadlo, A. Katrusiak, J. Phys. Chem. B 113 (2009) 13195.
[50] R. Gajda, A. Katrusiak, J. Crassous, CrystEngComm 11 (2009) 2668.
[51] K. Morokuma, J. Chem. Phys. 55 (1971) 1236.
[52] K. Kitaura, K. Morokuma, Int. Quantum Chem. 10 (1976) 325.
[53] H. Umeyama, K. Morokuma, J. Am. Chem. Soc. 99 (1977) 1316.
[54] D. Hadži, N. Kobilarov, J. Chem. Soc. A (1966) 439.
[55] S.E. Odinokov, A.A. Mashkovsky, V.P. Glazunov, A.V. Iogansen, B.V. Rassadin, Spectrochim. Acta 32A (1976) 1355.
[56] D. Hadži, S. Bratos, in: P. Schuster, G. Zundel, C. Sandorfy (Eds.), The Hydrogen Bond. Recent developments in Theory and Experiments, vol. 2, North Holland, Amsterdam, 1976, p. 565.
[57] W.F. Maddams, M.J. Southon, Spectrochim. Acta 38A (1992) 459.
[58] G. Talsky, Derivative Spectroscopy, VCH, Weinheim, 1994.
[59] Z. Dega-Szafran, A. Katrusiak, M. Szafran, J. Mol. Struct. 929 (2009) 182.
[60] D.A. Forsyth, A.B. Sebag, J. Am. Chem. Soc. 119 (1977) 9483.
[61] A.B. Sebag, D.A. Forsyth, M.A. Plante, J. Org. Chem. 66 (2001) 7967.
[62] I. Alkorta, J. Elguero, Magn. Reson. Chem. 42 (2004) 955.
[63] B. Ośmiałowski, E. Kolehmainen, R. Gawinecki, Magn. Reson. Chem. 39 (2001) 334.
[64] A. Katrusiak, J. Mol. Graph. Modelling 19 (2001) 363.